System identification for the Ott-Grebogi-Yorke controller design

Bogdan I. Epureanu and Earl H. Dowell
Department of Mechanical Engineering and Materials Science, Duke University, Durham, North Carolina 27708
(Received 17 July 1997)

A technique to compute the linearized Poincaré map and the sensitivity vector required for the implementation of an Ott-Grebogi-Yorke (OGY) controller from experimental data is presented. Unlike previous methods, the linearized map and the sensitivity vector are computed using only data collected over a single period of the limit cycle. The main advantage of the present method is the fact that it eliminates the long waiting period required to design an OGY controller using previously known methods. Numerical examples are presented using the Duffing oscillator with random perturbations to simulate noisy experimental data. [S1063-651X(97)10011-3]

PACS number(s): 05.45.+b

I. INTRODUCTION

Chaotic behavior, now commonly observed in a wide variety of laboratory experiments, is beginning to reveal its great potential for applications. One of the areas of significant practical relevance is the control of chaos. A successful attempt to control a chaotic system was made by Ott, Grebogi, and Yorke [1] and led to a wide variety of experimental validations [2–7]. Several researchers proposed various schemes derived from the original Ott-Grebogi-Yorke (OGY) method [8–13]. All these schemes are based on a linear analysis and control of the dynamics of the system in a Poincaré section and thus require the calculation of a linearized Pincaré map around a saddle node and a linear approximation of the motion of the saddle node due to variations of a control parameter referred to as a sensitivity vector.

Early examples of the control of chaos used maps known analytically, thus making the linearizations a straightforward step. Further investigations applied the OGY technique to nonlinear flows where the nonlinear Poincaré map was numerically computed and the linearized map and the sensitivity vector were easily obtained using finite differences. However, for experimental applications, the finite-difference technique usually cannot be used to compute the linearized Poincaré map since most physical experiments do not allow an arbitrary setting of the state space coordinates. However, the finite-difference technique can still be used to compute the sensitivity vector.

Most of the previous experiments computed the linearized Poincaré map using a linear least-squares fit of data measured in the Poincaré surface around the saddle node. To collect the required data, some researchers observed a trajectory of the system for a long period of time and acquired a pair of data points whenever the pair of state space locations were close to the saddle node. This acquisition scheme supplies data that belong to the strange attractor in the Poincaré map and are unevenly distributed around the saddle node because typically strange attractors do not have a uniform density of points. Therefore, this method gives good results for mildly unstable saddle nodes, but it may lead to large errors in the linear least-squares fit when severe instabilities are present [14]. To overcome this problem, Trickey [15] used a stochastic interrogation technique that allowed the acquisition of more uniformly placed state space locations. However, the stochastic interrogation did not eliminate the long waiting period required to collect the data.

In all the previous techniques used to implement OGY controllers, a long observation period is necessary to identify the system only after which can control be applied. In this paper we propose an alternative technique to compute both the linearized Poincaré map and the motion of the saddle node using a time series of the nonlinear system. In contrast to previous methods presented in the literature, the data necessary for the calculation are acquired along a trajectory that is close to the limit cycle that will be stabilized. We show that quite accurate results can be obtained using data collected during only one period of the limit cycle. The present technique thus allows the implementation of the OGY controller as soon as the system completes a cycle close to the limit cycle to be stabilized. Hence the present method eliminates the long waiting period required by previous techniques. The present method also allows the design of an adaptive controller that easily recomputes its parameters based on time series data, thus accounting for drifts in the parameters of the system [16].

One of the nonlinear flows most often studied in the literature, the Duffing oscillator [17–19], is used to demonstrate the present technique. Although the examples presented are numerical, the data are randomly perturbed to simulate experimental measurements.

II. SYSTEM IDENTIFICATION FROM A POINCARÉ SECTION

This section describes the nominal OGY method. In general, a nonlinear Poincaré map that depends on a parameter p and on the state space coordinate of the system $\mathbf{x}_n$ may be expressed as

$$\mathbf{x}_{n+1}=\mathbf{f}(\mathbf{x}_n,p). \tag{1}$$

The linear approximation of the map around a fixed point $\mathbf{x}_{\mathrm{FP}}$ for a nominal value of the parameter p_0 becomes

$$\mathbf{x}_{n+1}-\mathbf{x}_{\mathrm{FP}}\approx\mathbf{J}(\mathbf{x}_n-\mathbf{x}_{\mathrm{FP}})+\delta p\mathbf{w}, \tag{2}$$

where $\mathbf{J}$ is the Jacobian of $\mathbf{f}$, $\mathbf{J}=\partial\mathbf{f}/\partial x$, and $\mathbf{w}$ is the derivative of $\mathbf{f}$ with respect to p and is referred to as the *sensitivity vector* $\mathbf{w}=\partial\mathbf{f}/\partial p$. Both the Jacobian and the sensitivity vector are computed at the fixed point and at the nominal value of the parameter p_0.

The finite-difference approximation of the Jacobian may be calculated using state space coordinates that are close to the fixed point. For the case of a m-dimensional state space, a first-order accurate approximation of the Jacobian may be expressed as

$$\mathbf{J}\approx[\Delta\mathbf{f}_1\cdots\Delta\mathbf{f}_m][\Delta\mathbf{x}_1\cdots\Delta\mathbf{x}_m]^{-1}, \tag{3}$$

where $\Delta\mathbf{f}_i=\mathbf{f}(\mathbf{x}_{\mathrm{FP}}+\Delta\mathbf{x}_i,p_0)-\mathbf{f}(\mathbf{x}_{\mathrm{FP}},p_0)$ are column vectors and $\Delta\mathbf{x}_i$ are m linearly independent column vectors. Similarly, the sensitivity vector is approximated by

$$\mathbf{w}\approx\frac{\mathbf{f}(\mathbf{x}_{\mathrm{FP}},p_0+\Delta p)-\mathbf{f}(\mathbf{x}_{\mathrm{FP}},p_0)}{\Delta p}. \tag{4}$$

Alternatively, the Jacobian can be computed using a linear least-squares fit of data. In this technique the linearized Poincaré map in Eq. (2) is transformed to

$$\mathbf{x}_{n+1}\approx\mathbf{J}\mathbf{x}_n+\mathbf{b}, \tag{5}$$

where $\mathbf{b}$ is an unknown vector characterizing the fixed point $\mathbf{b}=x_{\mathrm{FP}}-\mathbf{J}\mathbf{x}_{\mathrm{FP}}$. An overdetermined linear system is then formed and solved using a standard linear least-squares solver. To compute the sensitivity vector one performs the linear least-squares fit twice, determines two fixed points for two values of the parameter p, and computes $\mathbf{w}$ using these two fixed points and Eq. (4).

The following example uses a two-well Duffing oscillator to show how a typical set of data may be acquired to identify the Jacobian corresponding to a period-one limit cycle. The nondimensional form of Duffing's equation, where the control parameter is the amplitude of excitation, may be expressed in first-order differential form as

$$\dot{x}=y,$$

$$\dot{y}=-\varepsilon y+\frac{1}{2}\frac{\omega_n^2}{\omega^2}(x-x^3)+p\,\cos(t+\varphi), \tag{6}$$

where ω_n and ε are the linear natural frequency and the nondimensional damping in both wells of the Duffing oscillator and ω, p, and φ are the frequency, the nondimensional amplitude, and the nondimensional phase of the excitation, respectively. The strange attractor displayed in a Poincaré section of the flow is shown in Fig. 1, where the circle indicates the region of radius 0.1 where the data were collected. A blowup of this region is shown in the upper right corner of Fig. 1. The distribution of the data around the fixed point is one of the critical aspects of the fitting technique. The banded structure of the attractor determines the distribution of the data because the data were collected by observing the motion of the system for many cycles and thus the states belong to the strange attractor. Consequently, there are large areas inside the circle of radius 0.1 that do not contain any data. This may lead to large inaccuracies for severely unstable fixed points because the data are stretched along the unstable manifold and contracted along the stable manifold thus being clustered along a curve. Kostelich has shown that this kind of structure leads to ill-conditioned least-squares problems [14] where the relative error in estimating the Jacobian is large even when the noise level in measurements is small.

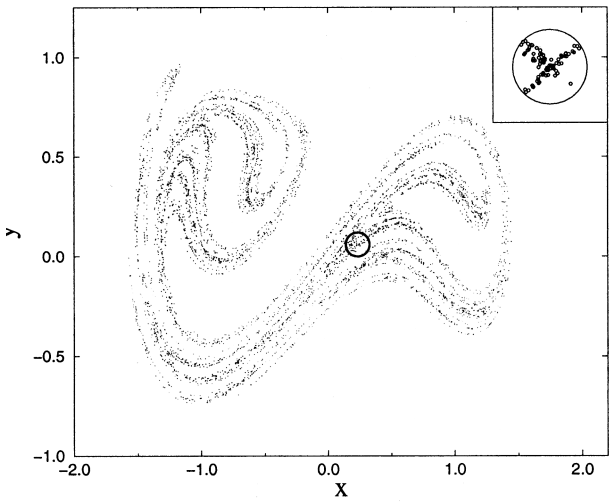

FIG. 1. Chaotic attractor obtained in a Poincaré section of Duffing's equation for $\varepsilon=0.0595$, $\omega_n=1$, $\omega=0.84$, and $p_0=0.2664$. The circle indicates the region of radius 0.1 centered at the saddle node. A blowup of this region is shown in the upper right corner.

III. SYSTEM IDENTIFICATION FROM A PERIOD OF THE LIMIT CYCLE

This section describes the proposed approach. The equation of a flow that has the Poincaré map given by Eq. (1) may be expressed in first-order differential form as

$$\dot{\mathbf{x}}=\mathbf{g}(\mathbf{x},p,t). \tag{7}$$

The linear approximation of $\mathbf{g}$ along the limit cycle $\mathbf{x}(t)=\mathbf{L}(t)$ that corresponds to $\mathbf{x}_{\mathrm{FP}}$ becomes

$$\dot{\mathbf{L}}+\delta\dot{\mathbf{x}}=\mathbf{g}\big|_{\substack{\mathbf{x}=\mathbf{L}(t)\\ \delta p=0}}+\frac{\partial\mathbf{g}}{\partial\mathbf{x}}\bigg|_{\substack{\mathbf{x}=\mathbf{L}(t)\\ \delta p=0}}\delta\mathbf{x}+\frac{\partial\mathbf{g}}{\partial p}\bigg|_{\substack{\mathbf{x}=\mathbf{L}(t)\\ \delta p=0}}\delta p, \tag{8}$$

where $\delta\mathbf{x}=\mathbf{x}(t)-\mathbf{L}(t)$ and $\delta p=p-p_0$. Transforming Eq. (8) into a linear system of ordinary differential equations with variable coefficients, one obtains

$$\delta\dot{\mathbf{x}}=\mathbf{A}(t)\,\delta\mathbf{x}+\mathbf{d}(t)\,\delta p, \tag{9}$$

where $\mathbf{A}(t)=\partial\mathbf{g}/\partial\mathbf{x}\big|_{\substack{\mathbf{x}=\mathbf{L}(t)\\ \delta p=0}}$ and $\mathbf{d}(t)=\partial\mathbf{g}/\partial p\big|_{\substack{\mathbf{x}=\mathbf{L}(t)\\ \delta p=0}}$. The solution of this system may be symbolically expressed as

$$\delta\mathbf{x}(t)=\exp\left(\int_0^t\mathbf{A}(\tau)d\tau\right)\delta\mathbf{x}(0)+\delta p\,\exp\left(\int_0^t\mathbf{A}(\tau)d\tau\right)\times\int_0^t\exp\left(-\int_0^\theta\mathbf{A}(\tau)d\tau\right)\mathbf{d}(\theta)d\theta. \tag{10}$$

The Poincaré section of the solution $\delta\mathbf{x}(t)$ leads to Eq. (2), where the Jacobian matrix is expressed as

$$\mathbf{J}=\exp\left(\int_0^T \mathbf{A}(\tau)d\tau\right) \tag{11}$$

and the sensitivity vector is given by

$$\mathbf{w}=\exp\left(\int_0^T \mathbf{A}(\tau)d\tau\right)\int_0^T \exp\left(-\int_0^\theta \mathbf{A}(\tau)d\tau\right)\mathbf{d}(\theta)d\theta, \tag{12}$$

where T is the period of the limit cycle to be stabilized. Consequently, only the matrix **A** is needed to compute the Jacobian **J**, while both **A** and **d** are need to compute the sensitivity vector.

To compute the matrix **A** we propose a method referred to as a *local identification*. This method assumes *a priori* a certain model for the real system and identifies the parameters that describe this model. The parameters are computed such that the state space trajectory of the model is close to the limit cycle of the real system. The *a priori* assumption of a model is not a rare situation but rather a generic one because approximate models may be developed for most systems of practical significance. Also the time-dependent part of **g** is generally due to the external excitation that is usually of known form. Furthermore, the model of the system is only required to be first-order accurate near the limit cycle for a single period T. Nevertheless, we note that generally it is not possible to determine a model that will accurately describe the real system for a long period of time due to the sensitivity to initial conditions. However, it is possible to approximate the dynamics of the system accurately for a short period of time as is needed for a local identification.

To demonstrate this method we consider a Duffing oscillator and its model given by

$$\ddot{x}=c_0\dot{x}+c_1x+c_2x^2+c_3x^3+c_4\cos(t)+c_5\sin(t). \tag{13}$$

Expressing Eq. (13) in a state space form and using a finite-difference scheme results in an equation at each instant of time t_i during a period T. For example, in the case of a constant time sampling interval, one may express the time derivative using a second-order approximation as

$$\mathbf{g}(\mathbf{x}_i,p_0,t_i)=\dot{\mathbf{x}}_i\approx\frac{\mathbf{x}_{i+1}-\mathbf{x}_{i-1}}{t_{i+1}-t_{i-1}}. \tag{14}$$

Equating the finite-difference value of **g** given by Eq. (14) with the expression given by Eq. (13), one obtains an overdetermined linear system of equations that is solved for the unknown parameters c_i. Since the flow has sensitivity to its initial conditions, a weighted linear least-squares solver needs to be used. The weighting is designed such that the errors in satisfying the equations obtained for large time values are more important than the errors in satisfying the equations obtained at small time values.

In Fig. 2 a time series of the simulated Duffing oscillator is shown by the dots. To simulate experimental data, the time series was randomly perturbed and a local identification was performed using the perturbed time series. The solid line indicates the trajectory of the identified model. As expected, the original and the identified systems have trajectories that are very close.

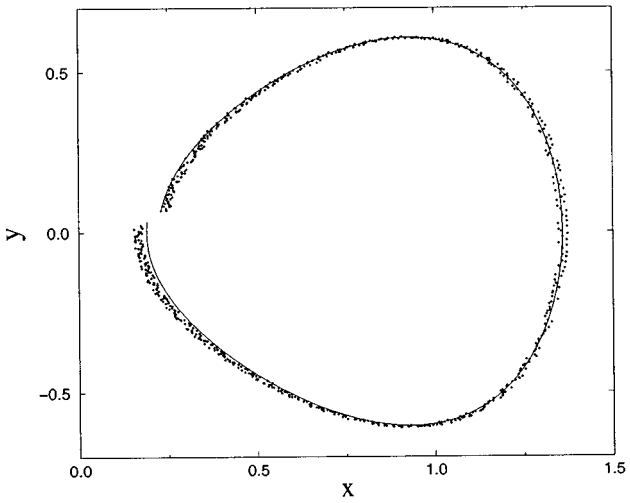

FIG. 2. The time series of the simulated Duffing oscillator is shown by the dots, while the solid line indicates the trajectory of the locally identified model given in Eq. (13).

Once the matrix **A** is computed, the Jacobian matrix is easily obtained using Eq. (11). One may also use Eq. (2) for $\delta p=0$ to determine the fixed point as

$$\mathbf{x}_{\mathrm{FP}}=(\mathbf{I}-\mathbf{J})^{-1}(\mathbf{x}_{n+1}-\mathbf{J}\mathbf{x}_n), \tag{15}$$

where **I** is the identity matrix and $\mathbf{x}_n$ and $\mathbf{x}_{n+1}$ are two adjacent states of the Poincaré map that represent the first and the last points of the time series.

To compute the sensitivity vector a second local identification for a different value of the parameter p is performed. The fixed point and **w** can then be found using Eqs. (15) and (4), respectively. This approach, however, requires the time series of two periods of the limit cycle, one for p_0 and the other for a different value for p. A different approach that uses data collected during a single period T is based on Eq. (12) where the vector **d** needs to be evaluated. Therefore, the form of the control excitation acting on the system has to be known. This situation is quite often encountered in practice because usually the external forcing is known. A typical example is the cosine function used in the driven Duffing oscillator shown in Eq. (6). For this type of forcing, the vector **d** is simply given by $\mathbf{d}(t)=[0\ \cos(t+\varphi)]^T$.

IV. NUMERICAL EXAMPLES

To simulate experimental measurements, Duffing's equations were integrated and then the state vectors were perturbed using a 0.013 maximum random perturbation of the position, a 0.003 maximum random perturbation of the velocity, and a 0.015 random perturbation of the location of a period one saddle node. The level of error introduced by the random perturbation was representative of the experimental results presented by Trickey [15].

The matrix **A** was computed using a local identification of the dynamics along the trajectory, while a vector **d** was considered of the form $\mathbf{d}(t)=[0\ \cos(t+\varphi)]^T$. The Jacobian, the sensitivity vector, and the fixed point location were then computed using Eqs. (11), (12), and (15), respectively. The results are presented in the first column of Table I and may

TABLE I. Numerical comparison of the three methods of system identification.

Parameter	Local identification	Linear fit	Exact	Error (%) local identification	Error (%) linear fit
$\mathbf{J}_{11}$	−2.35	−1.90	−2.27	3.40	16.36
$\mathbf{J}_{12}$	−4.44	−3.47	−4.21	7.67	11.14
$\mathbf{J}_{21}$	−1.35	−0.93	−1.18	14.13	20.77
$\mathbf{J}_{22}$	−2.91	−2.01	−2.49	16.74	19.17
$\mathbf{w}_x$	−5.12	−3.14	−4.44	15.21	29.20
$\mathbf{w}_y$	−2.74	−1.43	−2.04	34.50	29.88
x_{FP}	0.228	0.233	0.233	2.20	0.49
y_{FP}	0.0577	0.0597	0.0597	3.29	0.47
$\mathbf{q}_x$	0.476	0.628	0.544	12.4	15.4
$\mathbf{q}_y$	0.978	1.25	1.08	9.35	15.7

be compared with the results of a standard linear least-squares fit, which are shown in the second column of Table I. To simulate the noise in the system, the data used for the linear least-squares fit were randomly perturbed with the same level of perturbation as the time series used in the present technique. We also used a finite-difference scheme with *no perturbation* to identify the exact system and used those results as a reference for all the calculations. The exact values of $\mathbf{J}$, $\mathbf{w}$, and $\mathbf{x}_{\mathrm{FP}}$ are shown in the third column of Table I.

The OGY controller designed for a specific saddle node prescribes the amount of control parameter variation δp according to

$$\delta p = \mathbf{q}\Delta\mathbf{x}, \tag{16}$$

where $\Delta\mathbf{x}=\mathbf{x}-\mathbf{x}_{\mathrm{FP}}$ and $\mathbf{q}$ is a vector dependent on the Jacobian, the stable eigenvector, and the sensitivity vector. Consequently, the vector $\mathbf{q}$ has a critical influence on the control performance. Therefore, the global indicator of the quality of the OGY controller is given by the relative error in identifying $\mathbf{q}$. When we used the present identification technique and a sampling frequency of 700 points per period we obtained relative errors of 12.4% and 9.3% for the two components of $\mathbf{q}$. In comparison, the standard method led to relative errors of 15.4% and 15.7% when 50 pairs of state space locations in the Poincaré map were used.

V. DISCUSSION AND CONCLUSIONS

A different method to determine the linearized Poincaré map and sensitivity vector about a saddle node required for the implementation of an OGY controller was presented. The present technique is based on a model chosen *a priori* and a local identification of the nonlinear system that does not require a long period of time to observe the system in order to acquire data. The implementation of an OGY controller was shown to be possible as soon as the system completed only one orbit close to the limit cycle which is stabilized. This feature allows the design of an adaptive controller that accounts for parametric changes in the system. Accurate computations of both the Jacobian and the sensitivity vectors were shown for the particular case of a Duffing oscillator with random perturbations. Less than 13% relative error was obtained when a sampling frequency of 700 points per cycle was used.

There are several questions and observations that can be offered based upon the present work. For example, what is the sensitivity to the chosen radius of the identified region? Clearly, the radius of the region where the data are collected for the linear least-squares identification has a great influence on the results. On the one hand, the region should be small enough such that the linearity assumption is closely satisfied. On the other hand, the region should be sufficiently large to include enough points such that the measurement noise is small compared to the radius of the region. However, the problems that appear due to rapidly growing instabilities are not greatly affected by the size of the region as long as the region is small enough such that the linear approximations are valid. The more critical issue is that when rapidly growing instabilities are present the data are strongly clustered along the unstable manifold, which is locally a straight line. This clustering of the data leads to an ill-conditioned linear least-squares problem and large errors in approximating the Jacobian [14]. Of course, this issue is independent of the size of the region where the data are collected. When the instabilities are not severe, the clustering of the data is not so strong and the Jacobian may be accurately estimated.

What if the location of the fixed point is not known *a priori*? The present technique works better than the traditional method when the fixed point is not known. In the traditional method one first has to observe the system for a very long time and detect regions (very approximate regions) where the fixed points may be present. Then one makes a rough estimate of where the fixed pint may be located. Finally one collects data around the estimated fixed point and uses a linear least-squares fit to compute more precisely the fixed point and the Jacobian.

In contrast, the present technique virtually eliminates the waiting period when the system is only observed and no control can be applied. One scenario to apply the present technique is to observe the system until it undergoes a path that is almost closed (only one almost closed orbit). At that point one is able to compute the fixed point, the Jacobian, and the sensitivity vector. Therefore, once the system performs an almost closed orbit, one may start the controller.

In both the traditional and the present technique the fixed point need not be known *a priori*. The system is observed

and the fixed point is estimated based on the observations. The difference is that the present technique requires only one almost closed orbit, whereas the traditional technique requires several such orbits. For example, in the numerical example 50 such orbits were used for each calculation when the traditional method was used.

What if the nonlinearity and/or dimension of the system is not known? In this case the present technique cannot be directly applied. The drawback of the present technique is that it requires an *a priori* knowledge of the local behavior of the system close to the unstable orbit to be stabilized. The local identification cannot work if no local model for the system is available. However, for many physical systems of interest local models may be known. Moreover, only an approximate model is needed since a local identification is performed.

[1] E. Ott, C. Grebogi, and J. A. Yorke, Phys. Rev. Lett. **64**, 1196 (1990).
[2] W. L. Ditto and L. M. Pecora, Sci. Am. **269**, 78 (1993).
[3] W. L. Ditto, S. N. Rauseo, and M. L. Spano, Phys. Rev. Lett. **65**, 3211 (1990).
[4] M. Ding *et al.*, Phys. Rev. E **53**, 4334 (1996).
[5] T. L. Carroll, I. Triandaf, I. Schwartz, and L. Pecora, Phys. Rev. A **46**, 6189 (1992).
[6] E. R. Hunt, Phys. Rev. Lett. **67**, 1953 (1991).
[7] Y. C. Lai, M. Ding, and C. Grebogi, Phys. Rev. E **47**, 86 (1993).
[8] C. Reyl, L. Flepp, R. Badii, and E. Brun, Phys. Rev. E **47**, 267 (1993).
[9] S. Bielawski, D. Derozier, and P. Glorieux, Phys. Rev. A **47**, R2492 (1993).
[10] U. Dressler and G. Nitsche, Phys. Rev. Lett. **68**, 1 (1992).
[11] B. I. Epureanu, S. T. Trickey, and E. H. Dowell, Nonlinear Dynamics (to be published).
[12] P. V. Bayly, L. N. Virgin, J. A. Gottwald, and E. H. Dowell, in *Nonlinearity and Chaos in Engineering Dynamics* (Wiley, New York, 1994), Chap. 4.
[13] F. J. Romeiras, C. Grebogi, E. Ott, and W. P. Dayawansa, in *Chaotic Dynamics: Theory and Practice* (Plenum, New York, 1992), pp. 177–193.
[14] E. J. Kostelich, Physica D **58**, 138 (1992).
[15] S. T. Trickey, M. S. thesis, Duke University, 1997 (unpublished).
[16] J. P. Cusumano, D. Chelidze, and N. K. Hecht, in *Proceedings of the ASME Design Engineering Technical Conference* (DECT-ASME, Sacramento, 1997).
[17] D. W. Jordan and P. Smith, *Nonlinear Differential Equations* (Clarendon, Oxford, 1977).
[18] J. M. T. Thompson and H. B. Stewart, *Nonlinear Dynamics and Chaos* (Wiley, New York, 1986).
[19] J. A. Gottwald, L. N. Virgin, and E. H. Dowell, J. Sound Vib. **158**, 447 (1992).